

AI-enabled Welding Defect Detection and Resistivity Validation for Sustainable Manufacturing

Alvin Anderson, Guan-Yu Chen, and Shih-Chen Shi*

Department of Mechanical Engineering, National Cheng Kung University (NCKU),
No. 1, University Road, Tainan 70101, Taiwan

(Received October 10, 2025; accepted December 26, 2025)

Keywords: welding defect detection, deep learning, sustainable manufacturing, circular economy

Welding is a crucial process in manufacturing, but traditional inspection methods are slow, prone to errors, and labor-intensive. Automated detection using artificial intelligence offers a sustainable way to enhance efficiency and cut waste. In this study, we created an AI-driven framework to identify resistance spot welding defects by combining deep learning with experimental validation. ResNet18, ResNet50, UNet, and ResUNet were used to classify and segment weld images. Tensile testing pinpointed defective joints with stresses below 25 MPa, whereas resistivity tests showed that defective welds had a significantly higher electrical resistance. ResNet50 achieved the highest classification accuracy at 95%, and ResUNet provided the best segmentation with a mean Dice coefficient of 87%. These results show that combining AI with mechanical and electrical validation offers a reliable, efficient, and sustainable method for detecting welding defects. The proposed framework supports smart manufacturing and helps advance circular economy practices.

1. Introduction

Welding plays a crucial role in manufacturing automotive, electronics, and energy sectors, yet ensuring the reliability of welded joints remains a persistent challenge. Recent work has applied deep convolutional neural networks to classify welding defects from radiographic images, demonstrating the feasibility of image-driven inspection.⁽¹⁾ Automated detection using artificial intelligence offers a sustainable approach to improve efficiency and reduce waste. Deep-learning-based automated detection approaches have enabled the real-time identification of welding defects with improved efficiency and accuracy.⁽²⁾ Conventional defect inspection relies heavily on manual visual examination, which is subjective, time-consuming, and prone to human error.^(3,4) As product quality standards and sustainability requirements become increasingly strict, industries turn to automated inspection systems to improve efficiency, reduce costs, and minimize material waste.^(5,6) Deep-learning-based object detection techniques have also been applied to weld radiographs to locate and classify defects automatically.⁽²⁾ Recent

*Corresponding author: e-mail: scshi@mail.ncku.edu.tw
<https://doi.org/10.18494/SAM5977>

advances in artificial intelligence (AI) and computer vision have enabled the real-time detection of welding defects, addressing key challenges in sustainable production.⁽⁷⁾

Among these approaches, deep learning has become a powerful tool for image-based defect recognition and segmentation. Convolutional neural networks (CNNs), such as ResNet, have delivered superior classification performance by addressing the vanishing gradient problem through residual connections.⁽⁸⁾ Moreover, U-Net architectures are recognized for effectively capturing spatial features in semantic segmentation tasks.⁽⁹⁾ ResUNet has demonstrated improved performance in pixel-wise defect localization.⁽¹⁰⁾ Additionally, combining mechanical and electrical validation, such as tensile and resistivity tests,^(4,5) provides further insights into welded joints' structural and functional reliability, helping to align AI predictions with real-world manufacturing needs. Similar approaches have been reported in nanocomposites, where aluminum nanoadditives enhance both the mechanical and tribological properties of cellulose-based materials.⁽¹¹⁾ In addition, Al₂O₃ nanofluid lubricants modified with tannic acid and carboxymethyl have shown improved stability, superior anti-corrosive behavior, and enhanced tribological performance, further highlighting the importance of material-based validation for sustainable applications.⁽¹²⁾ Furthermore, studies on MoS₂/hydroxypropyl methylcellulose composite thin films have demonstrated that effective deagglomeration significantly improves tribological behavior, underscoring the role of microstructural control in enhancing surface durability and functional reliability.⁽¹³⁾

In this study, we hypothesize that combining ResNet and ResUNet architectures with experimental validation offers an accurate, efficient, and interpretable solution for detecting welding defects. We suggest that this dual approach achieves higher classification and segmentation accuracy, and uncovers the relationship among defect conditions, tensile strength, and resistivity, thereby advancing sustainable manufacturing practices.

2. Materials and Methods

2.1 Sample preparation and mechanical/electrical tests

Nickel-coated aluminum sheets (20 × 5 mm², thickness 15 μm) were resistant spot-welded at 1200 A. A stretching test was used to categorize the samples: welds with tensile stress ≥ 25 MPa were considered good, whereas those with tensile stress ≤ 25 MPa were classified as defective.⁽¹⁴⁾ Four-point probe (Kelvin method) resistivity measurements were performed to analyze the relationship between weld quality and electrical performance.

2.2 Image acquisition and dataset preparation

A Hayear 14 MP digital camera with a 180× C-mount lens was mounted on an aluminum extrusion frame to capture 1080 × 1080-pixel weld images. Eight hundred sixty-eight images were collected, with 365 good and 503 defective. Defective welds were manually annotated using LabelMe for segmentation. Data augmentation and fivefold cross-validation were applied, with 80% for training, 20% for validation, and 100 additional images for testing.

2.3 Deep learning models and training setup

For classification tasks, we employed ResNet18, ResNet50, and VGG16 architectures. Previous work used VGG16 transfer learning for welding defect classification with promising accuracy.⁽¹⁵⁾ The models were trained with binary cross-entropy loss, an Adam optimizer, a learning rate of 0.001, a batch size of 4, and 50 epochs. Segmentation tasks used UNet and ResUNet with Dice loss, an Adam optimizer, a learning rate of 0.001, a batch size of 8, and 100 epochs.

2.4 Performance evaluation

Classification accuracy and Dice coefficient were used to quantitatively evaluate the performance of the proposed deep learning framework for automated welding defect detection.

3. Results and Discussion

3.1 Mechanical evaluation of welded joints

Defective welds exhibit a rapid decline in stress, whereas good welds maintain higher stresses with stable deformation, as shown in Fig. 1. The threshold between acceptable and defective welds is set at 25 MPa, as summarized in Table 1.

3.2 Model training for weld classification

Deep learning models were trained to classify weld images, and their performance is illustrated in Fig. 2. ResNet18 and ResNet50 showed a faster convergence and a lower validation loss than VGG16, confirming their robustness. ResNet50 achieved the highest accuracy with 95% validation and 94% testing, as summarized in Table 2.

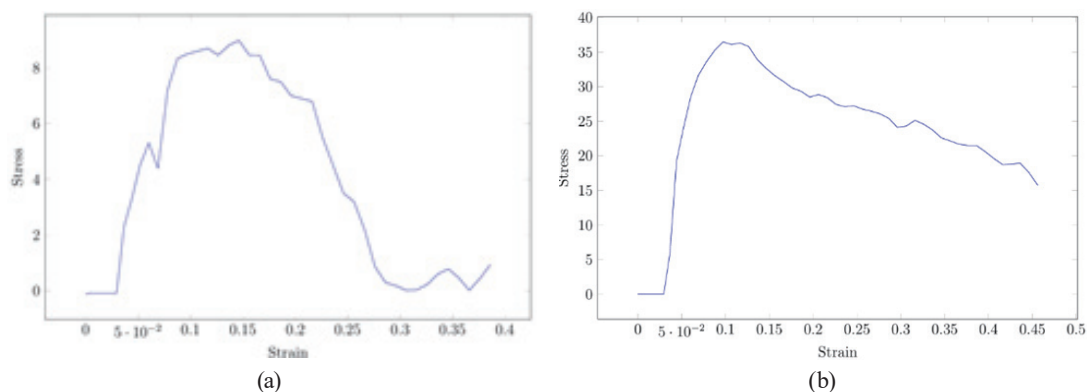


Fig. 1. (Color online) Stress–strain curves of weld joints: (a) defective weld showing premature fracture and (b) good weld showing stable plastic deformation.

Table 1
Tensile strength classification of welds.

| Condition | Stress |
|------------------------|-----------|
| Defective welding part | ≤ 25 |
| Good welding part | ≥ 25 |

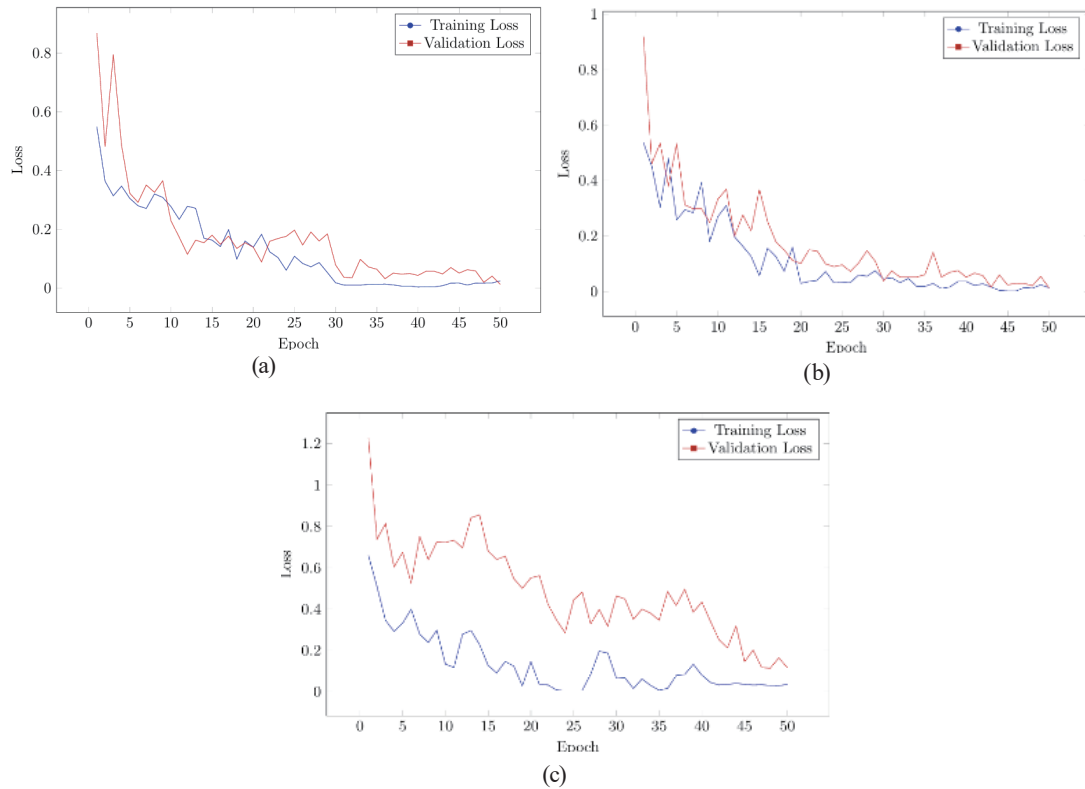


Fig. 2. (Color online) Training and validation loss curves of classification models: (a) ResNet18, (b) ResNet50, and (c) VGG16.

Table 2

Classification accuracy values of three deep learning models.


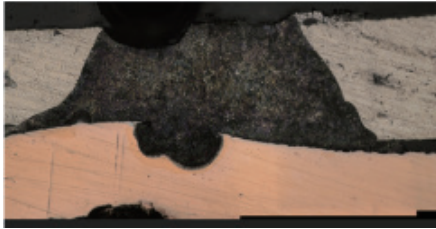
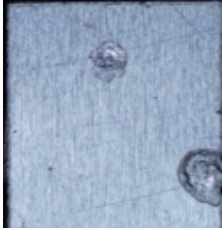


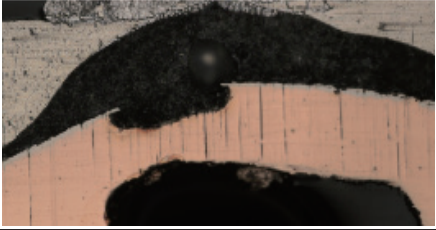


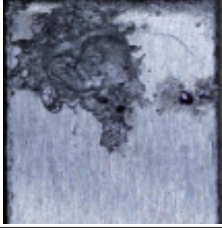
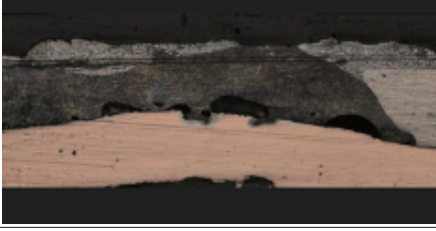
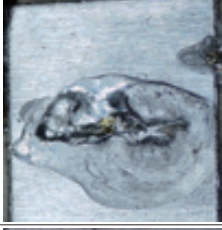
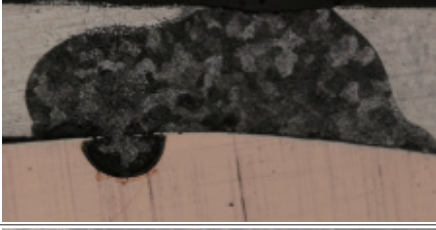
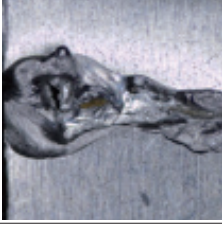
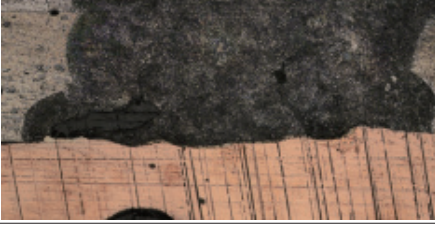
| Model | Validation accuracy (%) | Test accuracy (%) | GPU memory (GB) |
|----------|-------------------------|-------------------|-----------------|
| ResNet18 | 93 | 92 | 2.3 |
| ResNet50 | 95 | 94 | 3.5 |
| VGG16 | 87 | 84 | 2.1 |

As summarized in Table 2, ResNet50 consistently outperformed both ResNet18 and VGG16 in accuracy. ResNet18 still achieved stable classification with slightly lower accuracy, but used less GPU memory. These findings suggest that residual connections improve feature extraction, and deeper architectures offer only marginal benefits when sufficient training data are available.

3.3 Electrical resistivity as a validation tool

The four-point probe test was performed to confirm the electrical properties of the welds.⁽¹⁶⁾ Defective welds exhibited resistivity above 1000 Ω , whereas good welds showed values between 200 and 400 Ω . These results are summarized in Table 3, which shows the correlation between electrical resistance and weld integrity. Table 3 shows that abnormal resistivity in defective welds indicates poor bonding and incomplete fusion, with high values linked to voids and spatter at the joint interface. These results suggest that resistivity testing complements tensile evaluation by linking electrical behavior to weld quality. On the basis of these datasets, we assume that a resistivity of 1000 Ω is established as the threshold: welds measuring below 1000 Ω are classified as good and those at or above 1000 Ω are classified as defective.

Table 3
(Color online) Resistivity test results of good and defective welds.

| Sample | Image | Condition | Microscopy image | Resistivity (Ω) |
|--------|---|-----------|--|--------------------------|
| 1 |  | Good |  | 244.0 |
| 2 |  | Good |  | 389.4 |
| 3 |  | Good |  | 268.2 |
| 4 |  | Defective |  | 2072.4 |
| 5 |  | Defective |  | 3032.6 |
| 6 |  | Defective |  | 1688.9 |
| 7 |  | Defective |  | 2770.3 |

3.4 Segmentation for defect localization

Semantic segmentation was used to locate defect areas within weld images. Figure 3 illustrates that UNet converged with a higher validation loss, whereas ResUNet showed a smoother training progress. Their numerical results are summarized in Table 4, confirming that ResUNet outperformed UNet with a mean Dice coefficient of 87%.

3.5 Visualization of segmentation results

Table 5 shows the segmentation results. ResUNet generated clearer masks than UNet. Defect boundaries were captured with higher fidelity, enabling the accurate localization of irregular regions. This improvement indicates that residual blocks enhance the preservation of structural information during segmentation.

As summarized in Tables 4 and 5, classification and segmentation models demonstrate complementary performance. ResNet50 achieved the highest accuracy in classification, whereas ResUNet excelled at pixel-level defect localization. This integrated framework highlights the benefits of residual learning for both global and local feature representation.

3.6 Integrated framework for weld assessment

Integrating tensile tests, resistivity measurements, and AI-based models created a reliable inspection framework. As shown in Figs. 1–3, physical validation confirmed highly accurate model predictions. This multi-level approach ensures that classification and segmentation results are based on measurable mechanical and electrical properties.

The framework reduces rework and production delays by minimizing reliance on manual inspection. As shown in Tables 4 and 5, accurate defect detection prevented defective products

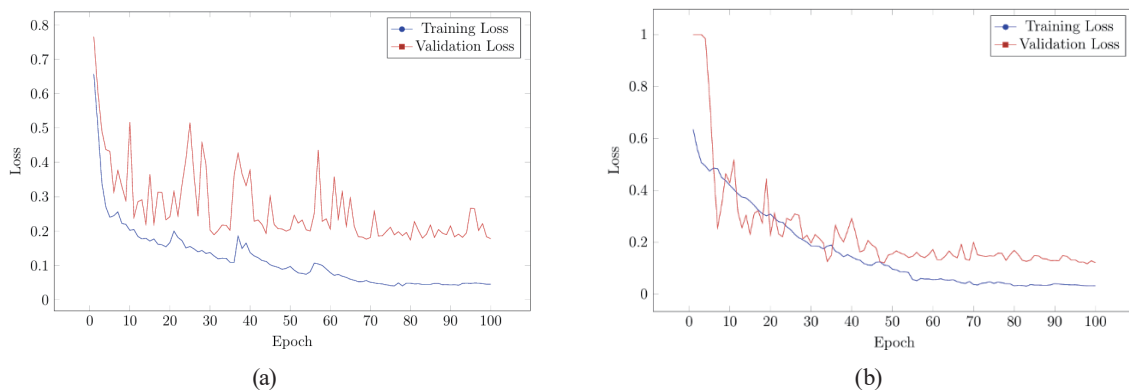
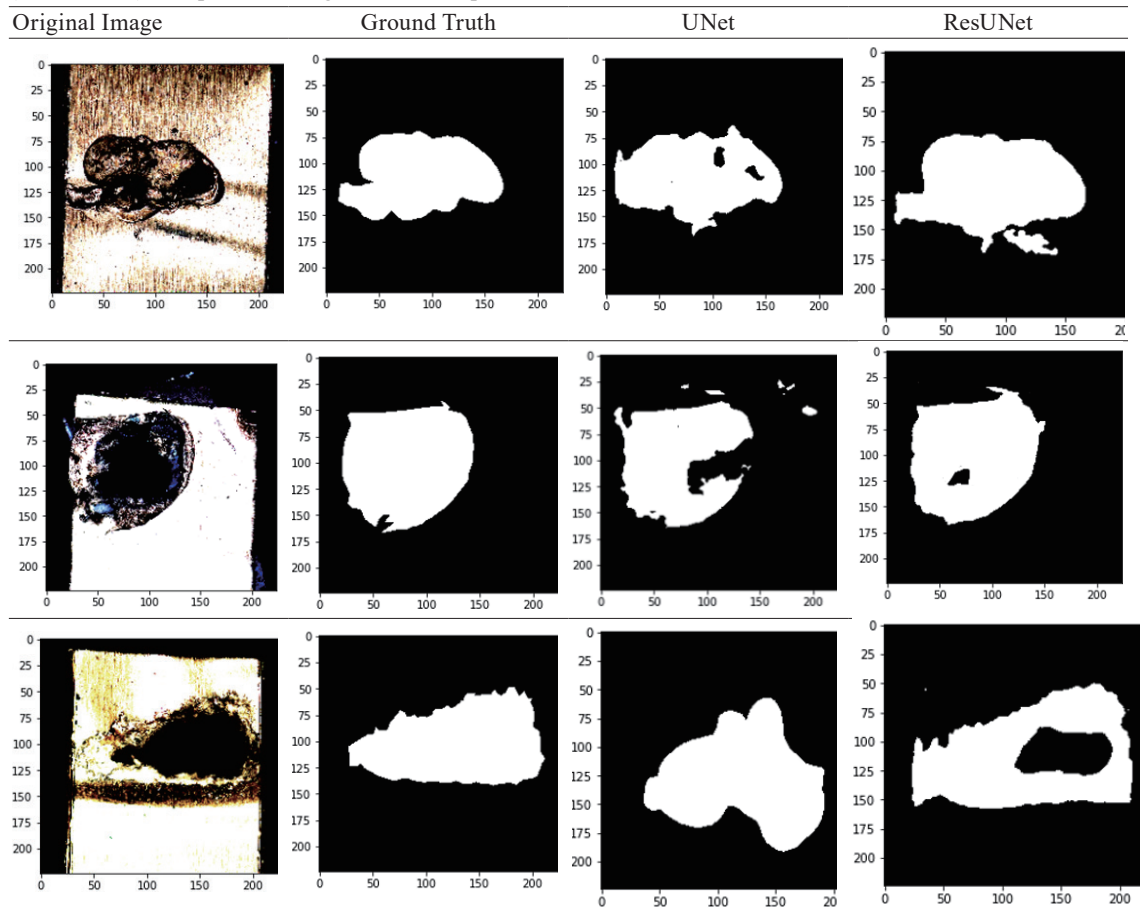


Fig. 3. (Color online) Training and validation loss curves of segmentation models: (a) UNet and (b) ResUNet.

Table 4
Segmentation performance of UNet and ResUNet models.

| Model | Mean dice score (%) | GPU memory (GB) |
|---------|---------------------|-----------------|
| UNet | 82 | 5.6 |
| ResUNet | 87 | 6.0 |

Table 5
(Color online) Comparison of segmentation outputs.



from progressing in the production line. This integration demonstrates a sustainable approach that conserves energy, materials, and labor resources.

Combining deep learning and sensor validation can go beyond welding inspection. Table 5 shows that defect localization can be applied to other manufacturing areas that need surface quality checks. These findings suggest that AI-driven systems can support circular economic practices across different industries.

In this study, we utilized two separate models for classification and segmentation, as summarized in Tables 4 and 5. Future research should investigate unified networks such as Mask R-CNN to improve efficiency. Integrating in real time with welding control can facilitate closed-loop optimization for more innovative and sustainable manufacturing.

4. Conclusions

In this study, we developed an automated framework for welding defect detection by integrating deep learning with experimental validation. Tensile tests showed defective welds fractured at low stresses, whereas good welds supported high loads with stable deformation.

Resistivity measurements confirmed that defective joints had a significantly higher electrical resistance than sound welds. Classification experiments revealed that ResNet50 achieved the highest accuracy and performed better than VGG16 in this study primarily because of its deeper architecture with residual connections (skip connections), which effectively address the vanishing gradient problem compared with VGG16. Moreover, segmentation tasks demonstrated that ResUNet offered a more reliable defect localization than UNet. Skip connections enhanced convergence and prevented vanishing gradients, although simpler architectures such as ResNet18 required less computational memory. This work provides a sustainable inspection approach that reduces manual effort, improves detection accuracy, and supports innovative manufacturing practices. Future research will focus on developing unified models capable of performing both classification and segmentation simultaneously, such as Mask R-CNN, and integrating these models with real-time process control to enable closed-loop optimization in advanced manufacturing environments. In addition, further investigations are needed to address key limitations, including insufficient dataset diversity, potential domain shifts when deployed in industrial settings, and the computational cost associated with real-time inference, to ensure the robustness and practical feasibility of the proposed approach

Acknowledgments

This work was supported by the National Science and Technology Council (NSTC), Taiwan (Grant Nos. 113-2221-E-006-087-MY2, 113-2221-E-006-112-MY2, and 114-2221-E-006-090). The authors acknowledge the Core Facility Center, National Cheng Kung University, for access to EM000600, funded under NSTC project 114-2740-M-006-001. Additional support from the Higher Education Sprout Project, Ministry of Education, through the Headquarters of University Advancement at National Cheng Kung University, is gratefully acknowledged.

References

- 1 D. Palma-Ramírez, B. D. Ross-Veitía, P. Font-Arriosa, A. Espinel-Hernández, A. Sanchez-Roca, H. Carvajal-Fals, J. R. Nuñez-Alvarez, and H. Hernández-Herrera: *Heliyon* **10** (2024) 30590.
- 2 W. Zhang, W. Liu, X. Yu, D. Kang, Z. Xiong, X. Lv, S. Huang, and Y. Li: *Coatings* **15** (2025) 808.
- 3 M. Amarnath, N. Sudharshan, and P. Srinivas: *Mater. Today: Proc.* (2023). <https://doi.org/10.1016/j.matpr.2023.03.268>
- 4 S. Gundewar, P. Kane, S. Behara, and U. Kumar: *IOP Conf. Series: Mater. Sci. Eng.* **1259** (2022) 012029.
- 5 Z. Zhang, Z. Yang, W. Ren, and G. Wen: *J. Manuf. Processes* **42** (2019) 51.
- 6 C. Zhu, H. Yuan, and G. Ma: *Mater. Res. Express* **9** (2022) 036503.
- 7 Y. Yang, L. Pan, J. Ma, R. Yang, Y. Zhu, Y. Yang, and L. Zhang: *Appl. Sci.* **10** (2020) 933.
- 8 K. He, X. Zhang, S. Ren, and J. Sun: *Proc. IEEE Conf. Computer Vision and Pattern Recognition* (2016) 770.
- 9 O. Ronneberger, P. Fischer, and T. Brox: *Int. Conf. Medical Image Computing and Computer-assisted Intervention* (2015) 234.
- 10 Z. Zhang, Q. Liu, and Y. Wang: *IEEE Geosci. Remote Sens. Lett.* **15** (2018) 749.
- 11 S.-C. Shi, T.-H. Chen, and P. K. Mandal: *Polymers* **12** (2020) 1246.
- 12 D. Rahmadiawan and S.-C. Shi: *Sci. Rep.* **14** (2024) 9217. <https://doi.org/10.1038/s41598-024-59010-w>
- 13 S.-C. Shi and J.-Y. Wu: *Surf. Coat. Technol.* **350** (2018) 1045.
- 14 M. S. Fakhri, A. Al-Mukhtar, and I. A. Mahmood: *Diagnostyka* **25** (2024).
- 15 P. S. S. Patchamatla, R. Riadhusin, N. S. Chandra, Pramodhini R, and K. Alagarraja: *Proc. 2025 3rd Int. Conf. on Integrated Circuits and Communication Systems (ICICACS)* (IEEE, 2025). <https://doi.org/10.1109/ICICACS65178.2025.10968402>
- 16 S.-C. Shi, W.-C. Weng, and D. Rahmadiawan: *J. Physics D: Appl. Phys.* **58** (2025) 105305.